Proceedings World Geothermal Congress 2000
Kyushu - Tohoku, Japan, May 28 - June 10, 2000

THE GEOPHYSICAL STRUCTURE OF THE LEYTE GEOTHERMAL PRODUCTION FIELD, PHILIPPINES

Nilo A. Apuada, Rhoel Enrico R. Olivar, David M. Rigor, Felixberto C. Maneja and Maribel C. Zaide-Delfin

PNOC-Energy Development Corporation, Fort Bonifacio Makati City, Metro Manila, Philippines 1201

Keywords: LGPF, Bouguer anomaly, velocity model, resistivity anomaly, micro-earthquake.

ABSTRACT

Various geophysical studies have been conducted at the Leyte Geothermal Production Field (LGPF). During the exploration and the early development stages, resistivity and gravity survey results were used to identify and site drilling targets. Seismic epicentral and frequency studies were also conducted to monitor the occurrence of micro-earthquake events before and during exploitation. Re-interpretation of these geophysical data and correlation with subsurface reservoir data allowed the characterization of two high temperature water-dominated geothermal systems in the LGPF.

Two different gravity signatures define the geothermal resources of LGPF. The Mahiao production field in the northwest is located inside the gravity high (2-6 mGals) while the Mahanagdong production field in the southeast is associated with the gravity low (<-2 mGals). The gravity high in the Mahiao production field is attributed to the combined effects of the Mamban Formation (MF) which is mainly composed of volcanic lava and breccias with very minor amount of sedimentary layers, and the Mahiao Sedimentary Complex (MSC) composed principally of conglomeratic microdiorite, quartz monzodiorite and volcanics. Furthermore, this field is defined by the 10 Ω-m anomaly that coincides with the upflow zone. The subsurface resistivity structure at about 500 meters depth exhibits an increasing resistivity value with depth. The formation of the low gravity anomaly in the Mahanagdong production field is due the presence of thick layers of (≈ 200 m) of siltstones and claystones found intercalating with MF and MSC. Based on drilling results, the upflow zone is associated with the 20 – 50 Ω-m resistivity gradient. However, this field is further manifested by the occurrence of two conductive zones (10 and 20 Ω-m closures) that signifies the outflow areas. Two-dimensional modeling reveals a decreasing resistivity values with depth.

Microearthquake monitoring before and during exploitation reveals that the earthquake activity at LGPF is dominated by the events occurring outside the geothermal field while the number of local events during the monitoring period remained fairly constant. The microearthquake activity at LGPF is associated with the Philippine Fault although induced seismicity was noted during injection and hydraulic experiment. The microearthquake low velocity (< 3.75 km/sec) model at 1.5-km depth correlates well with the 20 Ω-m resistivity contour and the hydrological flow pattern.

1. INTRODUCTION

The Leyte Geothermal Production Field (LGPF) is located at the central portion of the island of Leyte (Fig. 1). The area may be divided into six geographic sectors, namely: Mahiao, Sambaloran, Malitbog, Mamban, Mahanagdong and Bao valley. To date, LGPF has a total installed capacity of 699.4 MWe coming from the 112.5 MWe Tongonan I , 125 MWe Upper Mahiao, 231 Mwe Malitbog, 120 MWe Mahanagdong A, 60 MWe Mahanagdong B, and 50.9 MWe optimization power plants.

Various geophysical studies have been conducted at LGPF. From 1974 to 1976, KRTA (1977) conducted regional Schlumberger resistivity traversing (SRT) using fixed half-current electrode (AB/2) spacing of 250 and 500 meters. In addition, vertical electrical sounding (VES) measurements with maximum AB/2 equals to 1000 to 2000 meters were conducted during three field seasons: in 1981, 1983 and 1989-1990. In 1981, Ignacio and Bromley (1982) conducted baseline micro-gravity survey while Rigor and Bien (1987) performed epicentral studies in 1981 and 1983. Repeat gravity measurements and precise leveling survey were done in 1997 by Olivar and Apuada. Layugan et al. (1995) carried out baseline measurements for ground deformation using GPS and EDM and subsequently repeated in 1998. Maneja and Rigor made micro-earthquake studies in 1998.

This paper aims to characterize the geophysical signature of a water dominated high temperature geothermal system such as the LGPF.

2. RESULTS

2.1 Resistivity Survey

Schlumberger resistivity traversing (SRT) and vertical electrical sounding (VES) measurements delineated two distinct low resistivity anomalies defined by the apparent 20 Ω-m isoresistivity contour at AB/2 = 500 m (Fig. 2). The first anomaly encloses the acid-sulfate springs at Kapakuhan and the hydrothermally altered grounds at Mahiao, Sambaloran and Malitbog. The second anomaly covers the chloride springs at Bao and Banati, the acid-sulfate waters at Hanipolong, Paril and Mahanagdong and the bicarbonate spring at Malitbog river near Barangay Tongonan.

Based on 1-D modeling of the VES data, the two low resistivity anomalies in Figure 2 apparently merged at about 500-800 m interpreted depth (Fig. 3). The broad 20 Ω-m contour in Fig. 3 is open to the west towards the West fault line and encloses a well-defined mango-shaped 10 Ω-m closure along Mahiao-Sambaloran and the elongated 10 Ω-m contour in Bao-Mahanagdong sectors. Subsequent reinterpretation of the 1-D model reveals a pocket of 20 Ω-m at the southwestern part of the Mahanagdong sector.

The production and reinjection wells in Mahiao, Sambaloran and Malitbog sectors are mostly located inside the 10 Ω-m contour. However, subsequent step-out drilling revealed that the geothermal resource extends farther to the 30 Ω-m contour. On the contrary, most of the production wells in Mahanagdong sector are situated along the 20 - 50 Ω-m resistivity gradient, east of the 10 Ω-m contour. Well MG-7RD was initially drilled as a reinjection well and was later converted into a production well. It was formerly sited on a high resistivity (50-100 Ω-m) area but recent reinterpretation of the VES data suggested the presence of a 20 Ω-m contour.

The interpreted resistivity model depicted variable resistivity values (generally 1-50 Ω-m) at the last two segments of the resistivity layers (Fig. 4). Basically, the resistivity model at the Mahiao, Sambaloran, and Malitbog sector is characterized by low to moderately low resistivity strata (7-40 Ω-m) from surface to bottom. Except below VES stations V-16 and V-75 in the Upper Mahiao and Malitbog areas, respectively, the resistivity layers range from 3 to 3600 Ω-m. The varying resistivity values at shallow depth is due to the degree and intensity of alteration along the Mamban Formation (MF) and the Bao volcanics (BV). On the other hand, the resistivity feature in Mahanagdong sector is differentiated by relatively high resistivity values at the surface and second layers (70-6000 Ω-m). Likewise, the bottom resistivity layers are depicted by moderate to low resistivity values (8-50 Ω-m).

The contrasting resistivity values between the Mahanagdong and Mahiao geothermal systems are due to the varying composition and the degree of alteration in the MF and BV. In Mahanagdong, the BV is fresh to moderately altered and contains acid alteration minerals predominate. While in Mahiao, the BV and/or MF are moderately to intensely altered and host neutral fluids. Because of the limited depth of penetration of the VES method, no discernible resistivity signature could be derived for the Mahiao Sedimentary Complex (MSC) which occurs at an average depth of –900 meters.

The 10 Ω-m closure in Fig. 3 encompassing the Mahiao and Sambaloran production fields coincide with the location of the highest isothermal contour (Fig. 5). On the other hand, the Malitbog production field is situated along the gently increasing resistivity and decreasing temperature gradients. However, the Mahanagdong production field is related with the ill-defined 260°C isothermal contour which in turn lies within the 20-50 Ω-m resistivity gradient. The northwest-southeast trending elongated 10 Ω-m closure in the Bao valley correlates with the decreasing isothermal gradient (260-160°C).

2.2 Micro-earthquake Studies

Micro-earthquake studies in the LGPF commenced in 1980 with the establishment of a permanent seismograph station. In addition to the permanent station, five (5) temporary stations were installed during the short-period array studies in 1981, 1982 and 1987. Background occurrences of natural earthquakes were obtained for about two years before the 112.5 MWe Tongonan I power plant was constructed and operated commercially. During this period, the micro-earthquake events clustered along the strike-slip Philippine Fault Zone (PFZ) with depth of foci ranging from near surface to about 15 km. The largest magnitude as calculated from coda length was 2.4.

In 1997, the Institute De Physique Du Globe De Paris of France, together with PNOC-EDC and the Philippine Institute of Volcanology and Seismology (PHIVOLCS) installed a telemetered micro-earthquake monitoring network at the LGPF. The network had eighteen stations, and consisted of five of three component systems and thirteen sensors with single vertical component. The study aims 1) to detect possible increase in seismicity related to injection during power plant testing (before commissioning) of the additional 125 and 155 MWe in Upper Mahiao and Malitbog, respectively, and 2) to determine micro-earthquake events associated with hydraulic fracturing experiment (Maneja and Rigor, 1998).

One month before injection, seven of the twenty seven microearthquake epicenters lie outside of the production fields while the rest are distributed along the PFZ (Fig. 6). Only one epicenter plotted near the bottom of the injection well 5R8D. The pre-injection data suggest that LGPF is dominated by microseismic events not related to the geothermal exploitation.

During testing of the upper Mahiao and Malitbog power plants, 220 tons/day of geothermal fluids were reinjected at wells 5R1D, 5R4D, 5R5D, 5R8D, 5R3D and 5R7D. The calculated epicenters associated with this testing are mostly confined along the PFZ and at the bottom of wells 5R3D and 5R7D and their immediate vicinities (Fig. 6). Two weeks after the termination of the reinjection (also end of power plant testing), the network recorded a series of felt events. The epicenter of these events were generally located southeast of Mahanagdong along the Central Fault Line (Fig. 6).

Focal mechanism solution of the class A and B events along the PFZ was generated to determine the general direction of the fault movement. The solution indicates a left lateral strike-slip and dip-slip normal fault mechanism. Likewise, three-dimensional velocity modeling was made at -1500 meters depth (Fig. 7) with a background velocity of 3.75 km/sec. The modeling defined a tadpole-shaped low velocity (≤ 3.6 km/sec) anomaly. The north - south trending head of this low velocity anomaly occurs at the intersection of the East and Central fault line and covers the western sector of the Mahiao and Sambaloran production areas. The northwest-southeast trending tail of the anomaly, however, traverses the East and Central fault zones covering Malitbog, Mamban and part of Mahanagdong. This tadpole-shaped low velocity anomaly is surrounded by high velocity contours (> 3.8 km/sec) that are observed in Mahiao, Sambaloran, Bao and Mahanagdong areas. The high velocity contour in Bao valley coincides with the location of the serpentinite member of the Basement Complex that was intersected by well MG-3RD at –1300 meters.

The 300°C isothermal contour (Fig. 5) that represents the convective upflow encompassing wells 401, 410 and 209 in the Mahiao and Sambaloran areas is also related with the northeastern corner of the head of the low velocity contour (Fig. 7). The southeastern tail from Sambaloran to Mamban, on the other hand, correspond to the decreasing isothermal gradient, representing also the SE outflow based on geological, geochemical and reservoir data. The southern portion of the tail of the low velocity anomaly in Mahanagdong sector corresponds with the high temperature isothermal contour (290°C), while the high velocity contour in Bao is associated with the low temperature isothermal contour (240-260°C).

2.3 Gravity Survey

In 1982, Ignacio and Bromley identified two local positive residual anomalies with a magnitude of 18 – 24 mGals. The first anomaly (20-24 mGals) covers the Mahiao, Sambaloran, and Malitbog production sectors and the second (18-22 mGals) is situated in the Bao valley. These two positive anomalies were interpreted as a contiguous plutonic body that has been ruptured and offset about 4 km horizontally by left lateral movement along the Central Fault Line

The micro-gravity data in 1997 was processed to produce another Bouguer anomaly map and to generate 2.5-D models. The present data defined a distinct elongated positive anomaly oriented in an almost north-south direction (Fig. 8). It has a gravity value of 78 mGals that covers the Mahiao, Sambaloran, Malitbog and Bao areas. This central positive anomaly, likewise, identified four local positive anomalies (6 mGals) strategically located in Mahiao, Malitbog and Bao areas. A broader gravity high (> 78 mGals) also occurred outside of LGPF at the northeastern sector of the survey area. The eastern and western sides of the central positive anomaly are occupied by a well define negative gravity anomalies of 60 – 72 mGals. The Mahanagdong production field is found along the decreasing gravity gradient from Bao valley.

The configuration of the residual Bouguer anomaly (Fig. 9) closely resemble the Bouguer anomaly map except that the gravity value in the residual map is lower by 19% and the anomalies are clearly defined particularly at the Mahiao sector. In this map, the central positive anomaly is portrayed by the ≥ 2 mGals contour while the Mahanagdong is partially depicted by the ≤ -2 mGals contour and negative gravity gradient. Likewise, two negative anomaly (≤ -2 mGals) at the eastern and western side of Mahiao were also observed.

The most striking feature of the residual anomaly map is the occurrence of two smaller gravity high (>6 mGals) on the larger positive central anomaly (2 mGals). The first is a small pocket of >6 mGals contour at Malitbog. It is cut by several NW-SE trending faults such as the Litid North Fault, East Fault Line and Malitbog Fault. The West Fault Line likewise cuts the second and larger positive anomaly (6 mGals) which is located in Bao valley and extends towards the southwest. The Central Fault Line separates these two NE-SW trending local anomalies. Based on this figure, the NE half of the central positive anomaly is apparently related to the Mahiao, Sambaloran and Malitbog production fields which is bounded by the Central fault line to the west and the Litid north fault to the east.

The 2.5-D gravity modeling was constructed using the Geolink software. The background density which was used in the modeling is 2.5 g/cm^3. Two profile lines were chosen to illustrate the subsurface signature of the residual Bouguer anomaly. In the modeling, geologic well data were used to constrain the contact of different bodies with varying density. Location of profile lines is shown in Figure 8.

Profile line PO1 traverses the NE-SW trending southern part of the central anomaly along Bao and Malitbog areas (Fig. 10). The model resulted in a good fit between the observed and the calculated data. At the southwestern part, the model was constrained based on geological data from wells MG-3RD, 2RD and MN-1. The positive high, with amplitudes of >10 mGals represents the combined effect of the Basement Complex (BC), the Bao Volcanics (BV), Mahanagdong Claystone (MC) and the Mamban Formation (MF_1) with density values of 2.80, 2.50, 2.0 and 2.40 g/cm^3, respectively. The Mahiao Sedimentary Complex (MSC_1) with measured density of 2.70 g/cm^3 dominates the central portion of the section. The northeastern half positive anomaly, on the other hand, represents the effect of the BC, MSC and the MF_2 with lower density value (2.40 g/cm^3). Except for BV, the Mamban Formation (MF_1) with density value of 2.40 g/cm^3 was modeled overlying the BC, MC and MSC_1. The difference in density values of MF is due to their rock composition. MF_1 is composed mainly of volcanic lavas and andesite/dacite breccias with very minor amounts of sedimentary layers usually less than 10 meters thick while in MF_2 the volcanics are interlayered with about 200 m thick beds of fine-grained siltstone and claystone. The MSC_1, however, is composed mainly of conglomeratic microdiorite, quartz monzodiorite and volcanics with no recognizable sedimentary layers.

Profile line PO2 passes through the Mahiao, Sambaloran, Malitbog, Mamban and Mahanagdong production fields and is parallel to the direction of the positive anomaly (Fig. 11). The model is controlled by the well data from the five production sectors. The fit of the two gravity values at the northwestern half from well 405 to MN-1 is considered fair while a good fit was obtained at the southeastern half from MN-1 to MG-7RD. In general, the model is represented by occurrence of BV at the surface with an average thickness of about 300 meters. Underlying the BV is the MF_1 and MF_2 with an average thickness of 700 meters. Underlying $MF_1$and MF_2 are the MSC_1 and MSC_2.

3. DISCUSSION AND CONCLUSION

The geothermal system in LGPF is defined by two distinct resistivity and gravity signatures that represent two different geothermal system, such as, 1) the Mahiao, Sambaloran and Malitbog production field, and 2) the Mahanagdong production field.

Based on drilling results, the Mahiao, Sambaloran and Malitbog production fields are bounded by the 30 Ω-m contour and by more than 50 Ω-m contour particularly in the northern part of Mahiao area. The mango-shaped 10 Ω-m anomaly in the Mahiao and Sambaloran sectors represents the center of the geothermal resource as confirmed by the isothermal contour at -1000 meter rsl. This was also the area with highest chloride content and gradually decreases towards Malitbog. Likewise, this upwelling zone coincides to the northeastern corner of the head of the tadpole-shape microseismic low velocity contour (3.6 km/sec). The gradually decreasing resistivity and temperature gradient from Sambaloran to Malitbog and the southeast trending low velocity tail indicate the outflow pattern towards Bao valley.

The north-south orientation of the head of the low velocity contour also suggest an outflow signature from Mahiao to Bao valley. This flow pattern is likewise defined by isotope data where there is an increasing meteoric water dilution to the southeast from Mahiao to Sambaloran and towards Malitbog. This geothermal system is hosted by greater than 2 mGals positive residual gravity anomaly which was modeled as the MSC composed dominantly of conglomeratic microdiorite, quartz monzodiorite and volcanics lavas and breccias of the MF.

The Mahanagdong geothermal system, on the other hand, is located on the 20–50 Ω-m gentle gradient and distinguished by the presence of an elongated 10 Ω-m contour outflow signature from Paril to Bao valley. Geochemical data of the Bao-Banati springs and the fluids from TGE-4, TGE-5 and TGE-5A further suggest that these fluid is related to the Mahanagdong geothermal system (Alvis-Isidro et al). The southern part of the northwest-southeast trending low velocity tail together with the 280°C isothermal contour indicate the location of the upflow zone. Contrary to the first geothermal system, the Mahanagdong production field is hosted by less than –2 mGals negative gravity contours which was modeled as the less dense rock unit of MSC with density value of 2.45 g/cm^3 and is principally composed of about 200 meters thick layer of siltstone and claystone.

The gravity high (> 6 mGals) in Bao valley and Malitbog area were modeled as the impermeable pre-Tertiary serpentinites of the Basement Complex with a density of 2.80 g/cm^3. The gravity high in Bao valley was intersected by well MG-3RD at –1300 meters rsl.

The Mahanagdong claystone (MC) is reflected by the north-south trending negative gravity anomaly at the western side of Mahiao and the negative gravity tongue at the western part of Mahanagdong. It has an assigned density value of 2.30 g/cm^3. The MC was validated by 1R6D, MG-2RD and MG-10D drilling results.

SRT and VES delineated two geothermal systems distinctly portrayed by low and moderate resistivity values at the bottom layers. This contrasting resistivity value between Mahanagdong and Mahiao geothermal systems is due to the varying alteration composition and the degree of alteration in the MF and BV. In Mahanagdong, the BV is fresh to moderately altered and acid alteration minerals predominate. While in Mamban, the BV and/or MF are moderately to intensely altered and host neutral fluids.

Microearthquake studies revealed that the seismic events are related to the PFZ. Ground deformation study using EDM and GPS from 1991-1994 indicates that the West Block and the Central Block, the East Block and the Central Block and the West Block and the East Block of the PFZ have a slip rate of 1, 1.4 and 2 cm/yr, respectively. This horizontal movement is consistent with the rate of movement of the Philippine Fault.

ACKNOWLEDGEMENTS

We wish to thank the PNOC-EDC management for allowing us to publish the work presented in this report and to D.B. Layugan and F.G. Delfin for enlightening discussions and support in the fulfillment of this manuscript.

REFERENCES

Alvis-Isidro R. , R. R., Solana, R. R., D'Amore, F., Nuti, S., and Gonfiantini, R. (1993). Hydrology of the greater Tongonan geothermal system, Philippines, as deduced from geochemical and isotopic data. Geothermics. Vol. 22, No. 5/6, pp.435-449.

Apuada, N.A. (1994). Implication of the resistivity structure of central Leyte to Bato-Lunas and Anonang geothermal prospect. PNOC-EDC internal report, 60 pp.

Apuada, N.A. and Hallinan, S.E. (1994). Gravity models of the Mount Parker geothermal prospect, Mindanao. PNOC-EDC internal report, 12 pp.

Ignacio, C.P. and Bromley, C.J. (1982). Interpretation of gravitys at Tongonan geothermal field, northern Leyte, Philippines. PNOC-EDC Tech. Bull., 1, pp. 1-20.

KRTA. (1977). First stage report on geothermal exploration in Leyte. KRTA report, 59 pp.

KRTA. (1982). Tongonan geothermal field, Malitbog sector, data summary report. KRTA report, 25 pp.

Layugan, D.B., Catane, J.P.L., Maneja, F.C., Herras, E.B., and Vergara, M.C. (1990). Resistivity surveys across the Tongonan geothermal field, Leyte. PNOC-EDC internal report, 33 pp.

Layugan, D.B., Isada, M.G., Lumabi, P.S., Puertollano, J.R., Concepcion, J.A., and Siccion, R.C. (1995). Ground deformation study using electronic distance measurements in the greater Tongonan and Alto Peak geothermal fields, Leyte. PNOC-EDC internal report, 57 pp.

Maneja, F.C. and Rigor, D.M. (1998). Telemetered microseismic study of the grater Tongonan geothermal field. Proceedings of the 19th Annual PNOC-EDC Geothermal Conference, Makati City, Philippines, pp. 229-235.

Narag, I.C., Marte, B.F.C., and Valerio, A.R.A. (1993). May 17, 1993 Tongonan, Leyte earthquakes preliminary report of investigation. PHIVOLCS internal report, 17 pp.

Olivar, R.E.R. and Apuada, N.A. (1997). Baseline Microgravity and Precise Leveling Surveys, Leyte Geothermal Production Field. PNOC-EDC internal report, 16 pp.

PNOC-EDC. (1990). Resource Assessment-Grester Tongonan Geothermal Field. Part 1: Malitbog and Upper Mahiao sectors. PNOC-EDC internal report, 159 pp.

PNOC-EDC. (1993). Greater Tongonan Geothermal Field Integrated Resource Assessment. PNOC-EDC internal report, 231 pp.

Rigor, D.M. and Bien, O.C. (1987). Microearthquake studies in Tongonan Geothermal Field. PNOC-EDC internal report, 12 pp.

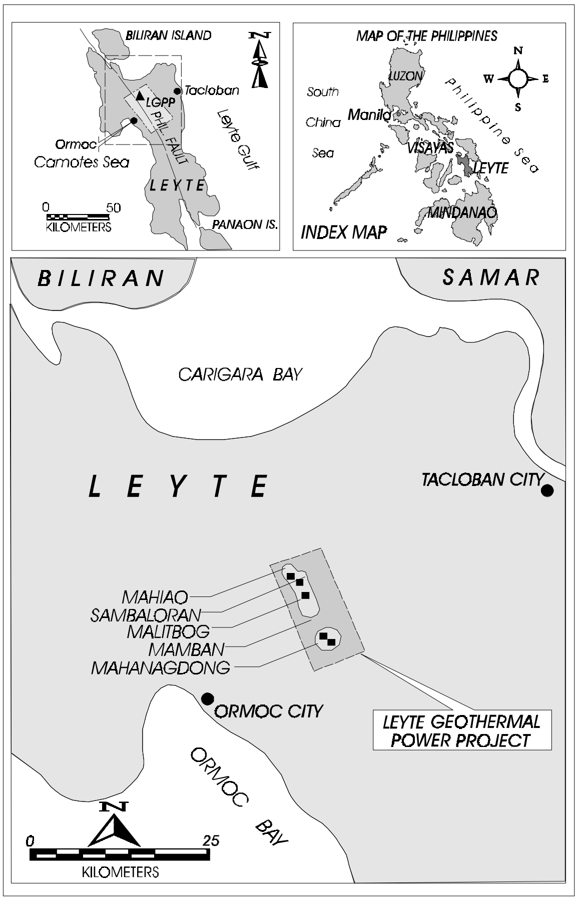

Figure 1. Location map of Leyte Geothermal Production Field.

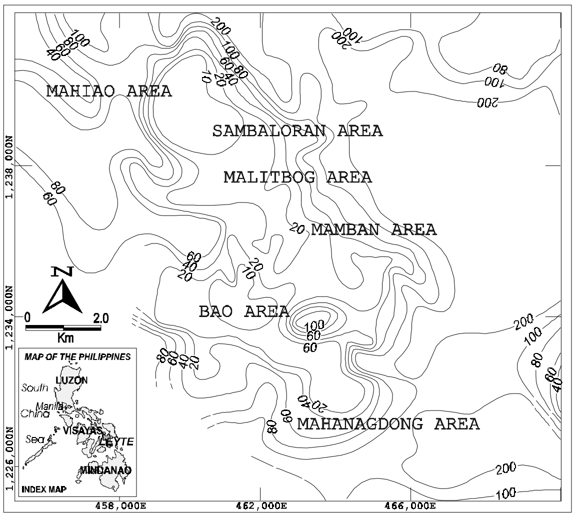

Figure 2. Apparent iso-resistivity map at AB/2 = 500 m.

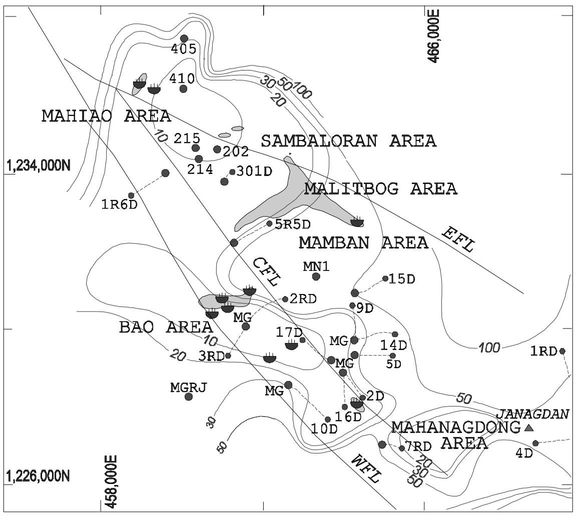

Figure 3. Iso-resistivity map at about 500 m depth based on VES.

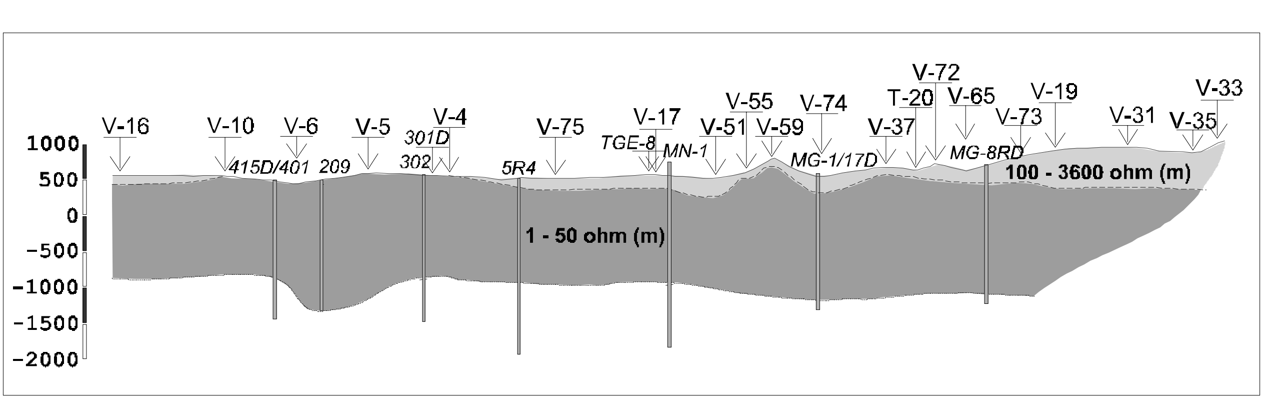

Figure 4. Resistivity model of Leyte Geothermal Production Field.

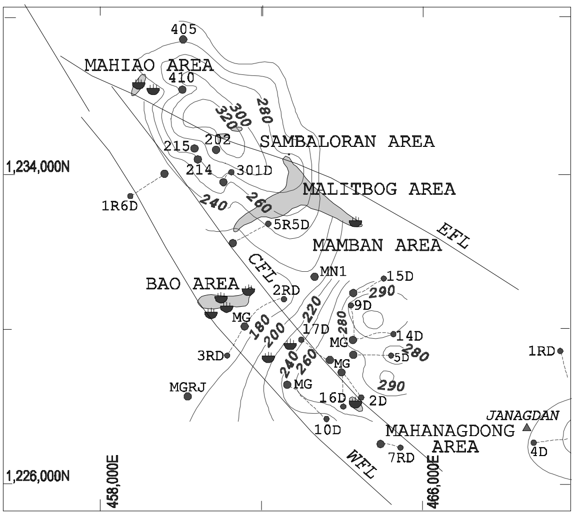

Figure 5. Isothermal contour at -1000 m.

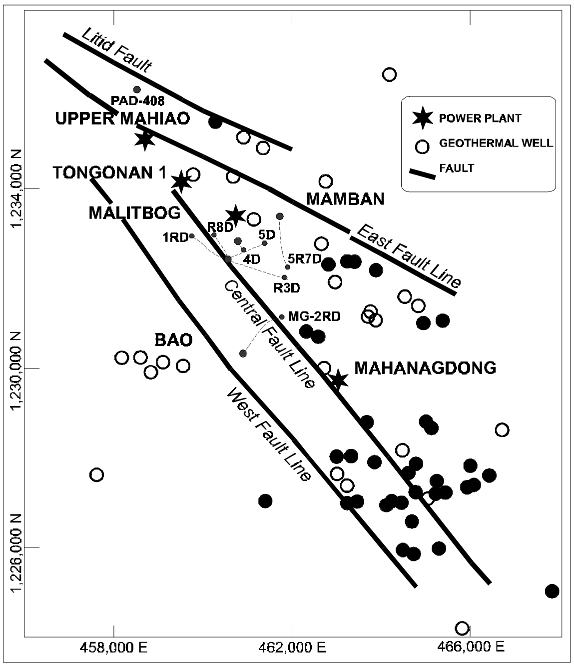

Figure 6. Distribution of micro-earthquake epicenter during power plant testing.

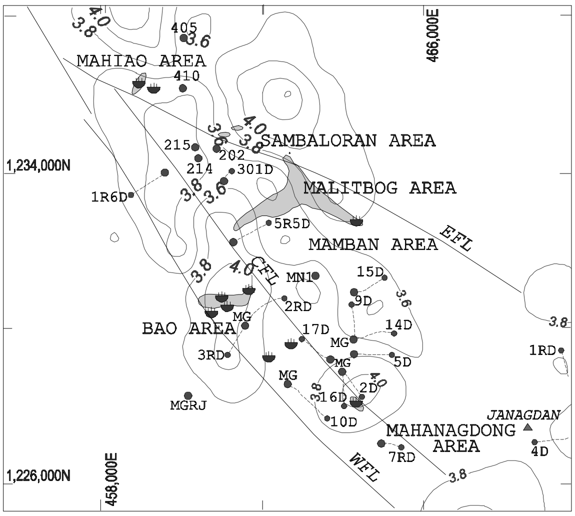

Figure 7. Iso-velocity map at -1500 meters depth.

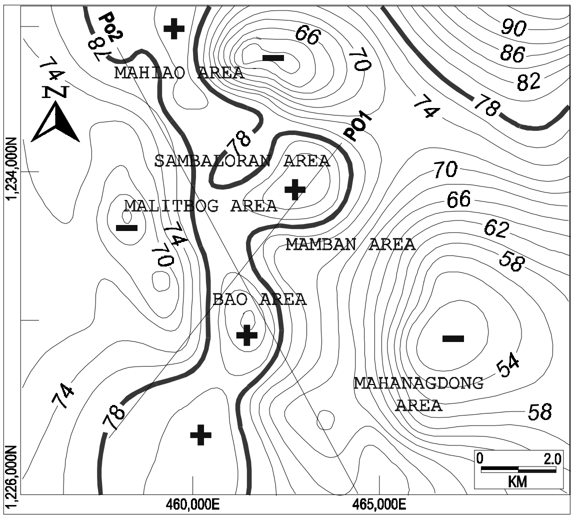

Figure 8. Bouguer gravity anomaly map.

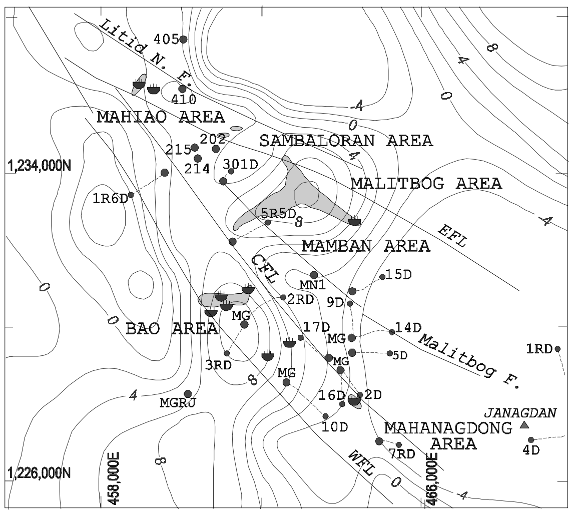

Figure 9. Residual Bouguer anomaly map.

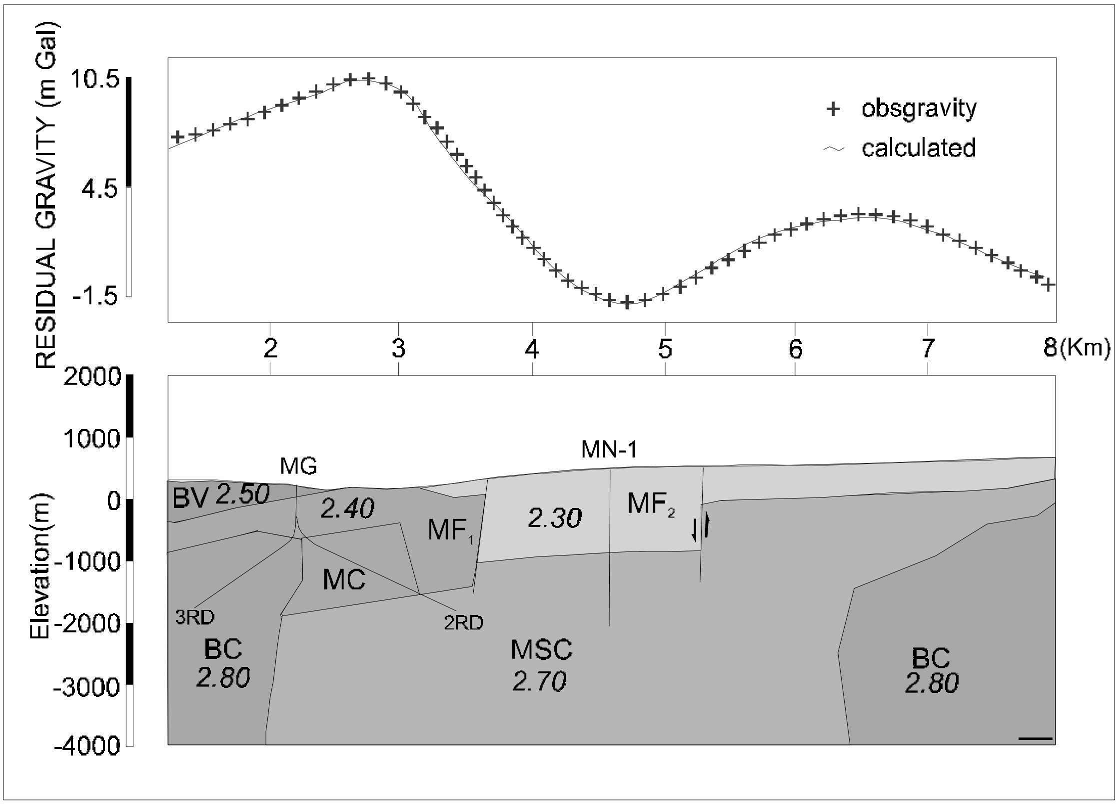

Figure 10. Gravity model along profile PO1.

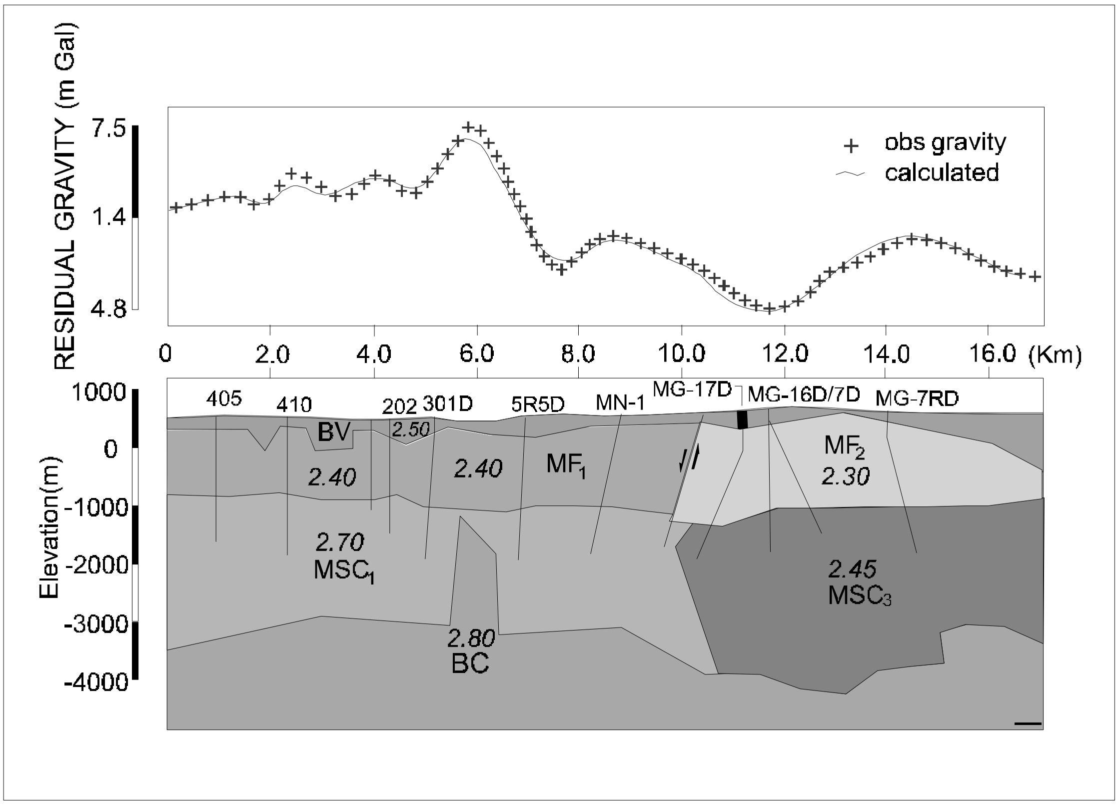

Figure 11. Gravity model along profile PO2